

Interband Transitions between Superdeformed Bands in ^{87}Nb : Evidence for a Superintruder Orbital

D. R. LaFosse,¹ M. Devlin,¹ M. Korolija,¹ F. Lerma,¹ D. G. Sarantites,¹ Y. A. Akovali,² C. Baktash,² C. J. Gross,² D. W. Stracener,² J. Döring,³ G. D. Johns,³ S. L. Tabor,³ F. E. Durham,⁴ I. Y. Lee,⁵ A. O. Macchiavelli,⁵ and W. Rathbun⁵

¹Chemistry Department, Washington University, St. Louis, Missouri 63130

²Physics Division, Oak Ridge National Laboratory, Oak Ridge, Tennessee 37831

³Department of Physics, Florida State University, Tallahassee, Florida 32306

⁴Department of Physics, Tulane University, New Orleans, Louisiana 70118

⁵Nuclear Science Division, Lawrence Berkeley National Laboratory, Berkeley, California 94720

(Received 9 October 1996)

Four superdeformed bands have been observed in ^{87}Nb . Transition quadrupole moment measurements on three of the bands confirm superdeformed shapes. Two of the bands were observed to mutually interact, and cross transitions between them have been observed. This is the first time such behavior has been observed in mass 80 superdeformed bands. Once this interaction is accounted for, a second crossing appears in one of the bands. This crossing is interpreted as evidence for the occupation of the $i_{13/2}$ superintruder orbital, making ^{87}Nb the lightest nucleus by far in which the shape-driving properties of this orbital can be studied. [S0031-9007(96)02263-6]

PACS numbers: 21.10.Re, 21.60.Cs, 23.20.Lv, 27.50.+e

The third generation of γ -ray detector arrays has greatly advanced the study of superdeformed (SD) nuclear shapes. However, the study of SD shapes in light nuclei near mass 80, beset by experimental difficulties [1], has benefited most from the new arrays. The GAMMASPHERE array paired with the MICROBALL [2] has been particularly successful. Whereas there were no SD bands known in this mass region two years ago, over 20 bands are now known. Multiple bands have been found in $^{80,81}\text{Sr}$ [3,4], $^{83,84}\text{Y}$ [5], and ^{83}Zr [6], and SD is known in other ^{38}Sr [1,7,8], ^{39}Y [9], and ^{40}Zr [10] nuclei.

The $N = 5$ $h_{11/2}$ intruder orbitals are of paramount importance to the stability of mass 80 SD shapes. These orbitals are lowered in energy with increasing deformation, and the Coriolis force lowers their energy further with increasing rotational frequency. Because of the low mass of these nuclei, SD bands possess very high rotational frequencies. Thus at the simultaneous extremes of deformation and rotation the $N = 6$ $i_{13/2}$ orbitals may also come into play [11]. These "superintruder" orbitals originate from one major shell higher than the $h_{11/2}$ intruders. Their shape-driving effects are well known in the mass 130 and 150 regions, but are, as yet, completely unknown in mass 80 nuclei.

This Letter reports on SD bands found in ^{87}Nb . Two SD bands have been found to mutually interact, and cross transitions between them have been observed. The identification of this interaction provides important information on the relative energies of nucleonic orbitals. In addition, a second single-particle crossing has been observed in one of the bands and is interpreted as evidence for occupation of the $i_{13/2}$ superintruder orbital.

High-spin states in ^{87}Nb were populated by the $^{58}\text{Ni}(^{32}\text{S}, 3p)$ reaction, using a 135-MeV beam provided

by the 88" cyclotron at the Lawrence Berkeley National Laboratory. The ^{58}Ni target had an effective thickness of $245 \mu\text{g}/\text{cm}^2$. The early implementation of GAMMASPHERE, consisting of 36 Ge detectors, was used to detect γ rays emitted by the residual nuclei. Emitted charged particles were detected by the MICROBALL [2], a 4π array of 95 CsI(Tl) detectors. A total of 4.2×10^8 events in which three or more Ge detectors fired in coincidence with one or more elements of the MICROBALL were accumulated.

The data from the MICROBALL was used to identify protons and α particles in each event; γ rays from events in which two or three protons and zero α particles were detected were sorted into E_γ - E_γ matrices and E_γ - E_γ - E_γ cubes. The proton energies were used to reconstruct the velocity vector of the recoiling nuclei, allowing an accurate event-by-event Doppler correction. The $4p$ and $\alpha 2p$ reaction channels were found to be present in the matrices and cubes. This contamination was removed by sorting $4p$ - and $\alpha 2p$ -gated matrices and subtracting a fraction of these from the original matrix. No such subtraction was performed on the cubes. In addition, the data were sorted into a directional correlation (DCO) [12] matrix to exploit angular correlations of coincident γ rays and determine multipolarities of some transitions. The DCO ratios were calibrated using transitions of known multipolarity; $E2$ transitions were found to have DCO ratios of ~ 1 , while unmixed dipole transitions had DCO ratios of 0.66 ± 0.05 .

Figure 1 shows the four SD bands which have been assigned to ^{87}Nb based on the three-proton requirement and coincidences with known low-spin transitions. The structures, labeled bands 1–4, were populated with relative intensities of $(2.0 \pm 0.2)\%$, $(1.9 \pm 0.2)\%$, $(3.2 \pm 0.3)\%$,

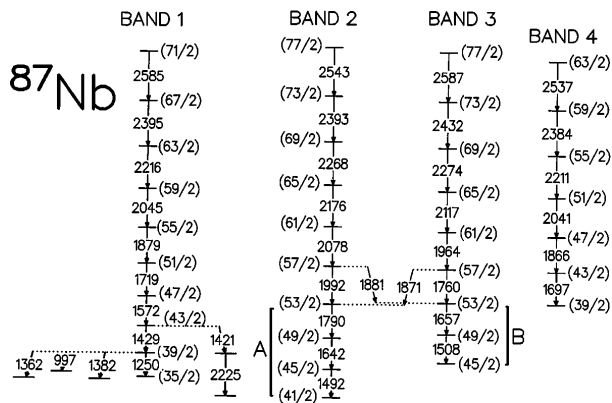


FIG. 1. Level scheme depicting the four SD bands in ^{87}Nb .

and $(1.3 \pm 0.3)\%$, respectively. DCO ratios measured for transitions of bands 1, 2, and 3 indicate that all have $E2$ character, excluding the weak uppermost transitions for which DCO ratios could not be measured. The reported spins of bands 1 and 2 were estimated as described in Ref. [1].

Finally, to determine that the bands represent SD shapes, a lifetime analysis of the SD bands was performed. The centroid shift method [13], as implemented in Ref. [10], was employed. The resulting values of the transition quadrupole moment (Q_t) were $Q_t = 5.2_{-0.8}^{+1.1} e b$ for band 1, $Q_t = 5.0_{-1.0}^{+0.7} e b$ for band 2, and $Q_t = 5.3_{-1.0}^{+1.2} e b$ for band 3. Assuming an axially symmetric shape, these values correspond to deformations of $\beta_2 = 0.50_{-0.07}^{+0.09}$, $\beta_2 = 0.49_{-0.09}^{+0.06}$, and $\beta_2 = 0.51_{-0.08}^{+0.10}$ for bands 1, 2, and 3 in order. These are comparable to $\beta_2 = 0.53$ measured for the SD band in ^{84}Zr [10].

The bands possess several interesting features, including the partial decay out of band 1, and cross-links between bands 2 and 3. This Letter focuses on bands 2 and 3; a full paper will discuss the four bands in detail.

As mentioned above, transitions were found which link bands 2 and 3. Evidence for such links can be seen in Fig. 2. Figures 2(a) and 2(b) show spectra representing bands 2 and 3, respectively. In the spectrum representing band 2, transitions from band 3 are apparent, and vice versa. Figure 1 shows the linking transitions and their place in the level scheme. Evidence that the coincidence relationships implied in Fig. 1 are correct is offered in Figs. 2(c)–2(f), where selected singly gated spectra are shown. These spectra illustrate that the level scheme shown in Fig. 1 is correct but possibly incomplete; the weak presence of the 1492-keV transition in the 1881- and 1760-keV gated spectra may indicate unobserved cross transitions. We estimate that any unobserved transitions have branching ratios less than 20%.

Thus the relative excitation energy of the bands is known. The relative spins and parities have been determined through the DCO ratios of the linking transitions. The DCO ratios of the 1992-, 1881-, 1871-, and 1760-keV

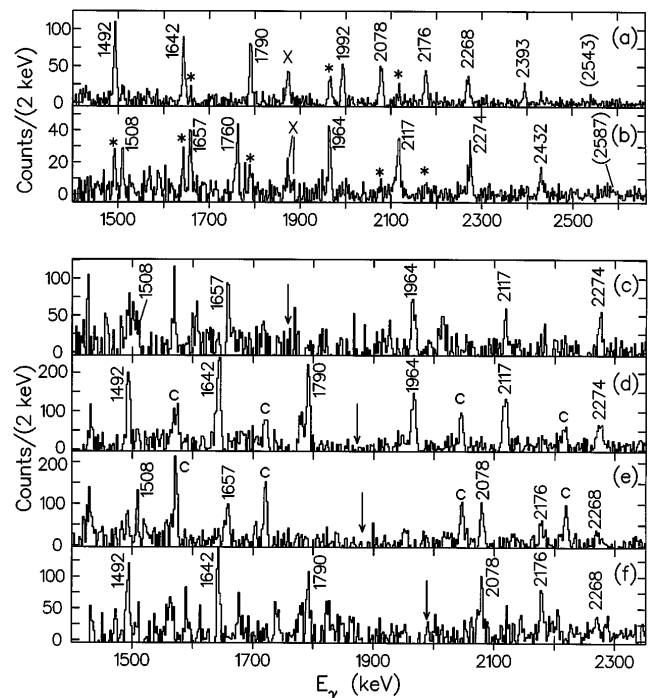


FIG. 2. Doubly gated spectra showing band 2 (a) and band 3 (b). Transitions from band 2(3) appearing in the spectrum representing band 3(2) are marked with an asterisk. Cross transitions between bands 2 and 3 are marked with the letter X. Frames (c)–(f) show single gates on the 1760-, 1871-, 1881-, and 1992-keV transitions; arrows indicate the gate energy. Contaminant peaks from the 1878-keV transition in band 1 are labeled with the letter C.

transitions were found to be, in order, 1.06 ± 0.16 , 0.89 ± 0.13 , 0.97 ± 0.17 , and 0.94 ± 0.12 . Thus we assign these transitions $E2$ character since mixed/nonstretched dipole transitions are unlikely and the spins of bands 2 and 3 are determined as shown in Fig. 1. This is one of the few times that the relative excitation energies, spins, and parities of two SD bands have been measured and the first such observation in the mass 80 region.

The linking of bands 2 and 3 can be studied further. Figure 1 shows that bands 2 and 3 cross each other; that is, band 2 is yrast for spins $I \leq 53/2\hbar$, while band 3 is yrast above $I = 53/2\hbar$. The dynamic moments of inertia ($J^{(2)}$) of the two bands, shown in Fig. 3, reveal pronounced irregularities at the point of the crossing. This behavior would be expected from two bands which mutually interact. Thus the interaction between bands 2 and 3 has been modeled using two-level mixing calculations. For the purpose of the calculations, it was assumed that the only pairs of interacting levels are those at $49/2\hbar$, $53/2\hbar$, and $57/2\hbar$. It was required that the calculations reproduce the measured branching ratios out of the $57/2\hbar$ states, and predict low-intensity cross transitions out of other levels, to explain the nonobservation of such links. Excellent agreement with experiment was obtained from an interaction strength $V_{\text{int}} = 42 \pm 1$ keV. The predicted

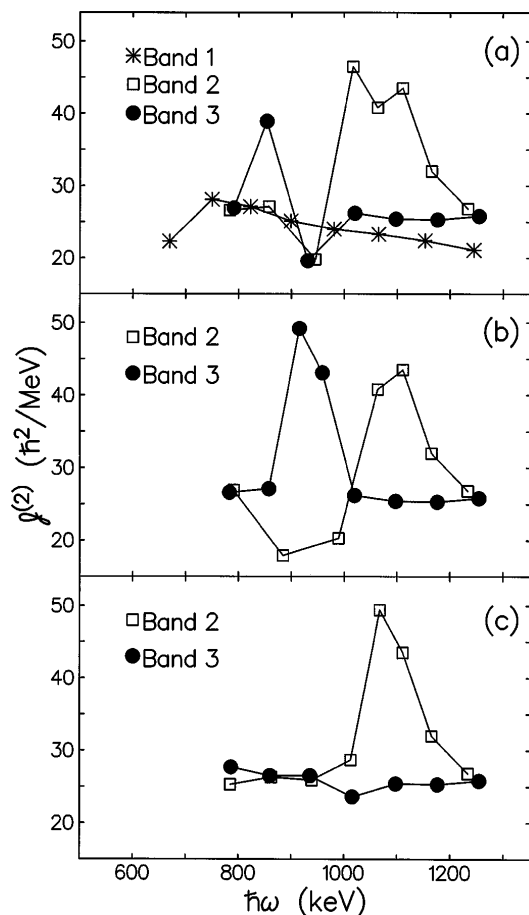


FIG. 3. (a) The dynamic moments of inertia ($J^{(2)}$) of bands 1, 2, and 3. (b) $J^{(2)}$ of bands 2 and 3 if sequences A and B (see Fig. 1) are swapped. (c) $J^{(2)}$ of bands 2 and 3 after the interaction between them has been removed. See text for details.

branching ratios for the 1881-keV (1871-keV) cross-band transition is 45% (60%), compared to the experimental value $(48 \pm 4)\%$ [$(55 \pm 6)\%$]. The most intense of the remaining predicted cross transitions has a branching ratio of 18%, just below the experimental level of sensitivity.

The interaction between bands 2 and 3 can now be removed from the data. The interaction between levels having the same spins perturbs the level energies by an amount given by $V_{\text{int}} = \frac{1}{2}\sqrt{(\Delta E_p)^2 - (\Delta E_u)^2}$, where ΔE_p and ΔE_u represent the perturbed (measured) and unperturbed energy spacings between pairs of levels. Using the unperturbed level energies, the $J^{(2)}$ of the bands has been recalculated as shown in Fig. 3(c). The flat $J^{(2)}$ of band 3 shows that the interaction between the bands has been removed. The $J^{(2)}$ of band 2 is now flat in the interaction region and displays a new feature: a peak at $\hbar\omega \approx 1.08$ MeV.

In order to understand the interaction between bands 2 and 3, cranked shell model (CSM) calculations have been performed. The results of such calculations using an axial

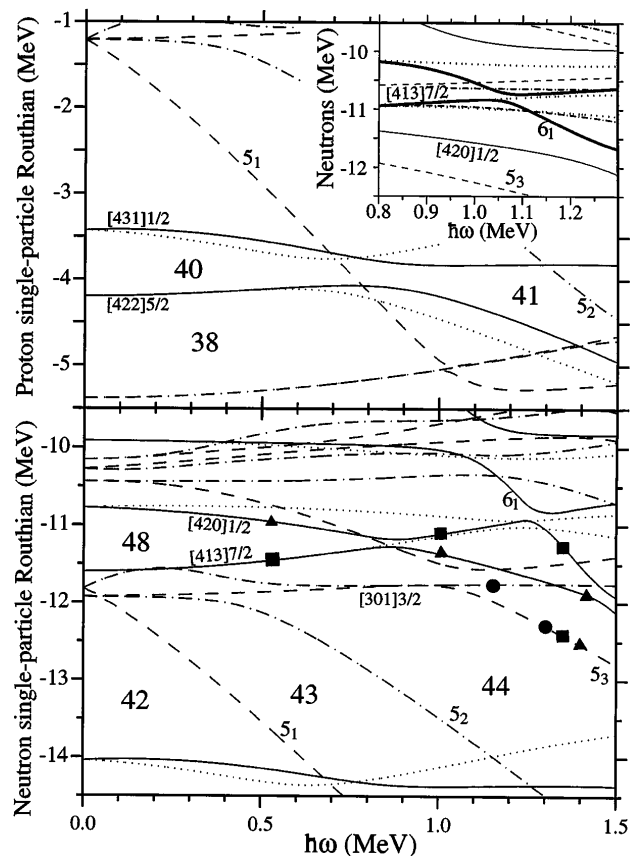


FIG. 4. CSM calculations performed with $\beta_2 = 0.50$. Relevant neutron/proton occupation numbers and single-particle orbitals are labeled. Some orbitals are marked according to the proposed configurations of bands 1–3. Circles represent band 1, squares band 2, and triangles band 3. Parity and signature of individual orbitals (π, α) are indicated as follows: solid lines (+, +); dotted lines (+, -); dashed lines (-, -); dash-dotted lines (-, +). Inset: CSM calculations for neutrons using $\beta_2 = 0.60$. The interaction between the 6_1 and $[413]7/2$ $\alpha = 1/2$ orbitals is highlighted.

deformation $\beta_2 = 0.5$ are shown in Fig. 4. The calculations suggest that bands 2 and 3 are neutron excitations to the $[413]7/2$ $\alpha = 1/2$ and $[420]1/2$ $\alpha = 1/2$ orbitals, respectively. These two orbitals cross at $\hbar\omega \approx 0.88$ MeV, with an interaction strength of $V_{\text{int}} = 47$ keV. These agree well with the experimental values $\hbar\omega = 0.93$ MeV and $V_{\text{int}} = 42 \pm 1$ keV. The only other crossing which occurs near the Fermi level and at approximately the correct rotational frequency is the $[431]1/2$ $\alpha = 1/2$ and $[422]5/2$ $\alpha = 1/2$ proton crossing. However, this crossing has a large interaction strength $V_{\text{int}} = 125$ keV and would have a small gradual effect on the $J^{(2)}$, rather than the large, abrupt effect which is observed.

As bands 2 and 3 are depicted in Fig. 1, their configurations do not change after the crossing. But, since the cross transitions have $E2$ character, the bottoms of the bands can be swapped; that is, sequence A becomes the bottom of band 3, sequence B the bottom of band 2. Drawn in

this manner the neutron configuration of band 2 would be $[420]1/2 \alpha = 1/2$ below the crossing and $[413]7/2 \alpha = 1/2$ above; the reverse holds for band 3. The $J^{(2)}$ of bands 2 and 3 now appear as shown in Fig. 3(b). The peak/dip at $\hbar\omega \approx 0.92$ MeV reflects the mixing between the bands as they cross and exchange character. The alignment gain of band 3 can be determined by integrating the peak in the $J^{(2)}$ [14]. The measured gain is $(2.0 \pm 0.3)\hbar$; the CSM calculations predict $1.8\hbar$. Thus the crossing between bands 2 and 3 is well understood.

The configurations determined for bands 1–3 are thus as follows. The bands possess identical proton configurations obtained by filling the single-proton orbitals up to the $Z = 41$ energy gap. The neutron configurations differ only in the orbital occupied by the final neutron. The neutron orbitals are filled up to the 5_3 level. Band 2 results from occupation of the $[413]7/2 \alpha = 1/2$ orbital, band 3 from occupation of the $[420]1/2 \alpha = 1/2$ orbital. Band 1, which shows no evidence of any crossings, is assigned the $[301]1/2 \alpha = 1/2$ orbital. These configurations are depicted in Fig. 4 with filled symbols.

The observation of two mutually interacting SD bands is rare. One example is found in ^{150}Gd [15], which was explained as an accidental degeneracy of two SD states in otherwise unrelated bands. Two interacting SD bands were observed in ^{193}Hg , explained as the crossing of two neutron orbitals [16]. However, ^{87}Nb is the first example where cross transitions between interacting bands have been observed. This provides valuable information regarding the relative positions of the $\nu[413]7/2 \alpha = 1/2$ and $\nu[420]1/2 \alpha = 1/2$ orbitals at SD shapes in the mass 80 region.

As mentioned previously, the removal of the interaction between bands 2 and 3 reveals a second interaction in band 2 at $\hbar\omega \approx 1.08$ MeV. Assuming the explanation of the interaction between bands 2 and 3 is correct, we propose that the second crossing is due to the crossing of the $i_{13/2}$ superintruder orbital and $[413]7/2 \alpha = 1/2$ neutron orbitals. Other crossings which are near the correct rotational frequency can be ruled out. For example, the crossing between the $[413]7/2 \alpha = -1/2$ and $[420]1/2 \alpha = -1/2$ neutron orbitals cannot be responsible, as neither orbital is occupied. The crossing between the $[301]3/2 \alpha = -1/2$ and 5_3 orbitals is too strong to be the cause of the observed sharp crossing and should be observed in bands 1, 2, and 3, rather than just band 2.

According to the CSM calculations, the crossing between the $i_{13/2}$ and $[413]7/2 \alpha = 1/2$ neutron orbitals is expected at a higher frequency than is observed. However, occupation of the superintruder orbital will drive the nucleus to a larger deformation. Neutron CSM calculations have thus been performed using a higher deformation, $\beta_2 = 0.6$, and are shown in the inset to Fig. 4. (Note that the method employed to measure the lifetimes is incapable of distinguishing the deformation change, given the statistical quality of the present data and the high

energies of the transitions involved.) At this deformation, agreement with experiment is much improved. The predicted crossing frequency is $\hbar\omega \approx 1.06$ MeV, compared to $\hbar\omega \approx 1.08$ MeV experimentally. Both the interaction strength of the crossing and the gain in alignment have been measured from the $J^{(2)}$ as in Ref. [14]. Experimentally, we measure $V_{\text{int}} = 70 \pm 10$ keV for this crossing in agreement with the predicted 75 keV. However, the predicted alignment gain is $\Delta i = 4.5\hbar$, whereas the measured value is $\Delta i = (2.6 \pm 0.4)\hbar$. This discrepancy may be due in part to the sensitivity of the alignment gain to the details of the nuclear shape parameters, including triaxiality and hexadecapole components, which have not been included. Also, it is apparent from Fig. 3(c) that the $i_{13/2}$ crossing begins below the $61/2\hbar$ level of band 2. The two-level mixing calculations discussed earlier did not include mixing with the $i_{13/2}$ orbital and assumed that the $61/2\hbar$ state of band 2 was purely $[413]7/2 \alpha = 1/2$. Thus the alignment gain measured for band 2 may not accurately reflect the true gain in alignment.

In summary, four new SD bands have been observed in ^{87}Nb . Linking transitions between two of the bands were identified; this is the first time the relative spins and excitation energies of two SD bands in a light nucleus have been experimentally determined. In addition, one of the two bands shows evidence for a crossing at high rotational frequencies. Evidence has been presented attributing this to the occupation of the $i_{13/2}$ superintruder orbital. Thus ^{87}Nb is the lightest nucleus by far in which the effects of this orbital have been observed.

Work supported in part by the U.S. D.O.E. under Grant No. DE FG05-88ER40406, by the U.S. N.S.F. under Grant No. PHY9210082, and by the Oak Ridge National Laboratory, managed by Lockheed Martin Energy Research Corporation for the U.S. D.O.E. under Contract No. DE-AC05-96OR22464.

-
- [1] D. R. LaFosse *et al.*, Phys. Lett. B **354**, 34 (1995).
 - [2] D. G. Sarantites *et al.*, Nucl. Instrum. Methods Phys. Res. Sect. A **381**, 418 (1996).
 - [3] M. Devlin *et al.* (to be published).
 - [4] F. Christancho *et al.*, Phys. Lett. B **357**, 281 (1995).
 - [5] H.-Q. Jin *et al.* (to be published).
 - [6] D. Rudolph *et al.*, Phys. Lett. B (to be published).
 - [7] C. Baktash *et al.*, Phys. Rev. Lett. **74**, 1946 (1995).
 - [8] A. G. Smith *et al.*, Phys. Lett. B **355**, 32 (1995).
 - [9] P. J. Dagnall *et al.*, Z. Phys. A **353**, 251 (1995).
 - [10] H.-Q. Jin *et al.*, Phys. Rev. Lett. **75**, 1471 (1995).
 - [11] A. V. Afanasjev and I. Ragnarsson, Nucl. Phys. A **586**, 377 (1995).
 - [12] K. S. Krane *et al.*, Nuclear Data Tables **A11**, 351 (1973).
 - [13] B. Cederwall *et al.*, Nucl. Instrum. Methods Phys. Res. Sect. A **354**, 591 (1995).
 - [14] V. P. Janzen *et al.*, Phys. Rev. Lett. **70**, 1065 (1993).
 - [15] C. W. Beausang *et al.*, Phys. Rev. Lett. **71**, 1800 (1993).
 - [16] D. M. Cullen *et al.*, Phys. Rev. Lett. **65**, 1547 (1990).